



Anti-citrullinated protein antibody B cells in rheumatoid arthritis: from disease-driving suspects to therapeutic targets

Kroos, S.

Citation

Kroos, S. (2026, February 10). *Anti-citrullinated protein antibody B cells in rheumatoid arthritis: from disease-driving suspects to therapeutic targets*. Retrieved from <https://hdl.handle.net/1887/4289572>

Version: Publisher's Version

[Licence agreement concerning inclusion of doctoral thesis in the Institutional Repository of the University of Leiden](#)

License: <https://hdl.handle.net/1887/4289572>

Note: To cite this publication please use the final published version (if applicable).



CHAPTER 7

Targeted depletion of autoreactive B cells using a bispecific complement engager

Sanne Kroos^{#1}, Sebastiaan M.W.R. Hamers^{#2}, Joanneke C. Kwekkeboom¹, Leendert A. Trouw³, René E.M. Toes^{*1}, Thomas H. Sharp^{*2,4}

¹ Department of Rheumatology, Leiden University Medical Center, Leiden, The Netherlands

² Department of Cell and Chemical Biology, Leiden University Medical Center, Leiden, The Netherlands

³ Department of Immunology, Leiden University Medical Center, Leiden, The Netherlands

⁴ School of Biochemistry, University of Bristol, Bristol, United Kingdom

* * These authors contributed equally

Abstract

Many autoimmune diseases are characterized by the presence of autoreactive B cells. For instance, rheumatoid arthritis (RA) is hallmark by B cells directed against the post-translational modification citrulline, also referred to as anti-citrullinated protein antibody (ACPA)-expressing B cells. Their proliferative status and ability to produce pro-inflammatory cytokines, together with the success of B cell depleting therapies in RA, point to the important role of ACPA-expressing B cells in disease pathogenesis. Current B cell-targeting therapies for RA deplete a large part of the B-cell compartment, thereby also impacting B cells not producing autoantibodies. To improve upon current therapies, we propose to specifically eradicate the ACPA-expressing B cells while maintaining the rest of the B-cell compartment. To investigate the possibility to specifically target and deplete autoreactive B cells only, we conjugated an anti-C1q nanobody to a citrullinated antigen and analysed its ability to recruit C1 to the ACPA-expressing B cells and mediate subsequent classical pathway-mediated cell lysis of autoreactive B cells specifically. Our data show the ability of this bispecific complement engager (BiCE) to induce complement-dependent cytotoxicity of B-cell lines expressing an ACPA B-cell receptor (BCR). Additionally, blocking of this cytotoxicity by soluble ACPA could be diminished by increasing the concentration of BiCE. Finally, we tested the BiCEs on patient-derived, ACPA-expressing B cell-containing PBMCs. Overall, we show that anti-C1q-CCP4 BiCEs have the potential to eradicate autoreactive ACPA-expressing B cells in a specific manner without affecting non-autoreactive bystander B cells.

Introduction

Many autoimmune diseases (AIDs) are driven by aberrant B cells recognizing self-antigens [1, 2], including rheumatoid arthritis (RA), as illustrated by the efficacy of B cell-targeting therapies [3]. RA is characterized by synovial tissue inflammation leading to swollen joints and bone erosions. A hallmark of RA is the presence of anti-citrullinated protein antibodies (ACPA) directed against the post-translational modification (PTM) citrulline [4]. ACPA are detectable years before disease onset and having ACPA-positive RA is correlated with more severe disease outcome [5], making their presence an important prognostic marker for disease progression.

ACPA-expressing B cells are implicated in the initiation and perpetuation of RA through multiple mechanisms, including the production of pro-inflammatory cytokines and the activation of other immune cell populations such as T cells [6-8]. In fact, the activated phenotype displayed by ACPA-expressing B cells is hypothesized to be part of the ongoing immunological activity in RA patients, since, even in clinical remission, the activated phenotype of ACPA-expressing B cells is retained [6, 7]. Suspected of fueling the chronicity of RA, selective elimination of these cells holds promise for achieving immunological remission.

Refining therapeutic strategies to selectively target antigen-specific B cells is crucial for developing more effective and potentially curative treatments while minimizing effects on non-target cells [1]. Currently available treatments for RA include rituximab, a chimeric monoclonal antibody [9]. By targeting CD20, rituximab eliminates CD20-expressing B cells through recruitment and activation of complement-mediated cytotoxic mechanisms [10]. However, this broad depletion negatively impacts the long-term immune protection and recall responses. Instead, we propose a more selective approach that targets the disease-specific ACPA-expressing B cells while preserving the broader B-cell repertoire.

To explore the possibility to deplete autoantigen-reactive B cells, we investigated bispecific complement engagers (BiCEs) in the context of ACPA-expressing cells. BiCEs selectively bind target cells via surface markers while simultaneously recruiting complement components to induce targeted cell lysis. Building on previous work demonstrating anti-C1q nanobody conjugates can mediate complement-dependent cytotoxicity in various contexts, including the elimination of HIV-infected cells [11-14], we have designed a BiCE that specifically targets ACPA-expressing B cells. We employed the anti-C1q nanobody C1qNb75, which has a proven ability to activate complement [12], and conjugated it to cyclic citrullinated peptide 4 (CCP4), a known B-cell receptor (BCR) ligand for ACPA-expressing B cells [15]. This enables complement activation selectively on the ACPA-expressing target B cells while minimizing off-target effects. As a negative control, we generated a variant in which C1qNb75 was linked to the arginine variant of the cyclic peptide (CArgP4). To our knowledge, the BiCE platform has not been previously applied to selectively deplete antigen-specific B cells, making our approach a novel strategy for targeted B-cell depletion. We made use of Ramos cell lines expressing an ACPA BCR, an anti-tetanus toxoid (TT) BCR or no BCR to evaluate the cytotoxic properties of C1qNb75-CCP4. Subsequently, we tested the killing properties of this BiCE on ACPA-expressing B cells in peripheral blood mononuclear cells (PBMCs) derived from ACPA⁺-RA patients. Altogether, we show the potential of this BiCE platform to antigen-specifically eradicate autoreactive B cells.

Materials & Methods

Protein expression

The nanobody constructs were ordered via Genscript and the cloning procedure was performed using standard restriction enzyme cloning procedures. Constructs were inserted into a pCPF3.05 plasmid. Enzymes and ligation kits were ordered from NEB. The expression was performed using BL21-DE3 bacteria grown at 37°C with continuous agitation at 200 rpm. Cells were grown to an OD600 of 0.6 in lysogeny broth, and then 0.5 mM of Isopropyl β -D-1-thiogalactopyranoside (IPTG) (VWR chemicals, NL) was added to induce protein synthesis. Protein expression was performed at 20°C for approximately 16 hours, after which cells were pelleted and lysed in cold wash buffer. Wash buffer constituted 300 mM NaCl, 20 mM Tris-HCl (pH 8) and 20 mM imidazole. Cells were lysed using probe sonication, and debris was subsequently removed by centrifugation at 24 000g for 40 minutes at 4°C. HisPurTM Ni-NTA beads were used to purify the protein constructs. Columns were equilibrated with wash buffer, and then wash buffer with increasing imidazole concentrations was added iteratively until the imidazole concentration reached 250 mM. SDS-PAGE analysis confirmed that the protein constructs had been expressed and purified.

Protein-peptide conjugation

Purified proteins were buffer exchanged from the Ni-NTA purification wash buffer to sortase buffer using dialysis with 12 000 MW cutoff dialysis sacks (Sigma Aldrich). The sortase buffer contained 150 mM NaCl, 50 mM Tris (pH 7.4) and 10% glycerol. A GGG-DBCO peptide (BroadPharm) was dissolved in sortase buffer and conjugated to C1qNb75 constructs using sortase A. The molar ratios were 20 equivalents peptide and 0.5 equiv. of sortase A. The reaction was performed for 1 hour at RT with C1qNb75 at 15–50 μ M, depending on the protein expression yield. Samples were then immediately loaded onto a Ni-NTA column to separate any unreacted product and the Sortase A, since the HisTag was C-terminal to the sortag on each construct this was essentially an inverse strategy to Tag-based purification. Then samples were dialyzed against PBS to get rid of all unreacted GGG-DBCO peptide. Subsequently, the azide-modified peptide was conjugated to the C1qNb75 protein constructs at 2 molar equivalents. The samples were analysed by SDS-PAGE and mass spectrometry.

For SDS-PAGE, samples were prepared using Laemmli sample buffer with 1 mM DTT, heated to 95°C for 5 minutes and loaded onto a 4–12% pre-cast Bis-Tris Protein Gel. The running buffer consisted of 20 mM MOPS free acid (pH 7), 5 mM sodium acetate and 1 mM disodium EDTA (MOPS buffer), 0.1% SDS. Electrophoresis was performed at 200 V for 35 minutes on a Mini-PROTEAN Tetra Cell electrophoresis device (Bio-Rad), followed by Coomassie-blue staining of the gels.

Mass spectrometry analysis was conducted by first running the protein samples over a UPLC Protein C4 column (2.1x50 mm). The eluents A and B consisted of ultrapure water with 0.1% formic acid (A) and acetonitrile with 0.1% formic acid (B). The samples were maintained at 60°C, and the gradient of B was ramped from 2% to 95% over 5 minutes. Then a Waters Xevo G2-XS QTOF mass spectrometer, which uses electrospray ionization, was used to obtain the mass data from 50–2000 m/z . The m/z data were then deconvoluted to obtain the mass peaks.

Cell lines

For functional testing of the BiCEs, Ramos cells expressing an ACPA-BCR (3F3 IgG1, 7E4 IgG1, 2G9 IgG1, 1B8 IgM, 3F3 IgG3), expressing an anti-TT-BCR (D2 IgG1) or expressing no BCR (MDL-AID KO) were used [15]. The B-cell lines were cultured in RPMI1640 (Gibco), 8% FCS, 100 U/ml penicillin/streptomycin and 2 mM GlutaMAX (Gibco) at 37°C, 5% CO₂.

Patient material

Peripheral blood samples were obtained from six ACPA-positive RA patients through the outpatient clinic of the Department of Rheumatology at Leiden University Medical Center (LUMC). All participants fulfilled the 2010 ACR/EULAR classification criteria for RA at the time of diagnosis. The study was approved by the LUMC ethical review board (protocol P17.151), and all patients provided written informed consent. Participants were either receiving therapy with methotrexate, hydroxychloroquine, sulfasalazine and/or leflunomide (Supplementary Table 2).

Cell viability assays

To investigate the effects of the BiCEs on cell viability, XTT assays were performed. Ramos cells were plated in 96-wells flat bottom culture plates (Corning) at a density of 200.000 cells/well in CDC medium (RPMI1640 (Gibco) + 0.1% BSA). Rituximab (Rixathon) or BiCEs were diluted in CDC medium containing 10% normal human serum (NHS). Plates containing the Ramos cells were subsequently centrifuged (5 min 300g RT), supernatant was removed and the cells were resuspended in the diluted BiCEs. In eculizumab experiments, 100 µg/mL eculizumab was added to the medium containing NHS and the diluted BiCEs before addition to the cells. In monoclonal antibody/plasma blocking experiments, diluted BiCEs were pre-incubated with indicated amounts of monoclonal antibody or plasma for 30 min on ice, before addition to the cells. Plates containing the cells and treatments were incubated for 1 hour at 37°C, 5% CO₂. Thereafter, XTT reagents (Sigma Aldrich) were added and incubated for another 4 hours at 37°C, 5% CO₂. Absorbance was measured at 450 nm in a Biorad ELISA reader. Background signal (from wells containing CDC medium only) was subtracted and OD450 values were normalized to wells containing cells and CDC medium only.

Ramos anti-IgG/anti-IgM staining

Ramos cells derived from the same culture as used during the XTT viability assays were stained with anti-IgG or anti-IgM to evaluate the levels of BCR expression. Cells were washed twice in FACS buffer (PBS 1% BSA) and plated in 96-wells V-bottom plates at a density of 200.000 cells/well. Subsequently, the plate was centrifuged (5 min 300g 4°C) and cell pellets were resuspended in 40µL staining solution containing anti-IgG-BV421 (BD Biosciences #562581) or anti-IgM-PerCP-Cy5.5 (BioLegend #314512). Samples were incubated for 30 min at 4°C and subsequently washed twice in FACS buffer. Finally, the samples were resuspended in 100µL PFA and acquired on BD LSRII Fortessa. Samples were analyzed using OMIQ software.

Ramos CCP4-tetramer staining

The efficacy of the BiCEs was also tested by performing BCR stainings with labeled CCP4 tetramers. CCP4 tetramers were produced as described previously, but in short, biotinylated CCP4 was conjugated to streptavidins labeled with brilliant violet 605 (BV605) or allophycocyanin (APC) [15, 16]. Ramos 3F3 IgG1 cells were spiked into healthy-donor derived PBMCs from buffy coats (10.000 Ramos cells

into 5 million PBMCs) and the cell mixture received BiCE treatment in the same way as described in XTT viability assays. After incubation, cells were transferred to a V-bottom plate and centrifuged (5 min 300g RT). Thereafter, cells were stained and measured as described in section 'viability assays patient derived cells'.

When evaluating the effect of eculizumab, Ramos cells expressing no BCR (MDL-AID KO) were mixed with Ramos 3F3 IgG1 cells in a 1:1 ratio. After receiving BiCE (+/- eculizumab) treatment the same way as described in XTT viability assays, cells were stained with CCP4-APC and CCP4-BV605 tetramers and measured on a Cytek 3L Aurora flow cytometer.

Viability assays patient-derived cells

PBMCs from RA patients were isolated using Ficoll-Paque gradient centrifugation and immediately used for subsequent steps. For collection of complement-active autologous serum, within 30 min after blood withdrawal, a serum tube was kept on ice for one hour to let the blood clot. Thereafter, serum was collected and kept on ice until usage.

PBMCs were split into two samples: one was incubated with C1qNb75-ta-CCP4 in presence of 10% NHS or 10% autologous serum, the other was incubated with C1qNb75-ta-CCP4 in presence of 10% heat-inactivated NHS (30-60 min 56°C) or 10% heat-inactivated autologous serum. Per 15 million PBMCs, 1µM of C1qNb75-ta-CCP4 in 100 µl of CDC medium containing 10% (heat-inactivated) serum was added, in Eppendorf tubes. Samples were resuspended well and incubated for one hour at 37°C 5% CO₂ in an overhead roller. Thereafter, 1 mL PBS 1% BSA was added to the tubes and cells were transferred to 15 mL tubes, which were centrifuged (500g 5 min 4°C). Samples were resuspended in Fixable Viability Dye eFluor506 (Invitrogen) and incubated for 30 min on ice in the dark. Cells were subsequently washed twice with PBS 1% BSA and incubated for 5 min on ice in the dark in Cytofix fixation buffer (BD Cytofix #554655, 2x diluted in PBS) on ice. After this fixation step, cells were washed twice in PBS 1% BSA and incubated in an extracellular staining mix for 30 min at RT (CD3-eFluor506 (UCHT1, Invitrogen), CD14-eFluor506 (61D3, Invitrogen; the dump channel consisted of Fixable Viability Dye, CD3 and CD14), CD19-BV570 (HIB19, BioLegend), CD27-APC-Fire810 (QA17A18, BioLegend), CD38-BV785 (HIT2, BioLegend), IgD-APC-Fire750 (IA6-2, BioLegend), IgG-BV421 (G18-145, BD), CCP4-APC, CCP4-BV605, CArgP4-BV711. After incubation, cells were washed twice in PBS 1% BSA (700g 5 min 20°C) and resuspended in 1% paraformaldehyde, which was incubated for 15 min at RT. Finally, cells were resuspended in PBS 1% BSA and stored at 4°C until measurement on a Cytek 3L Aurora flow cytometer.

Results

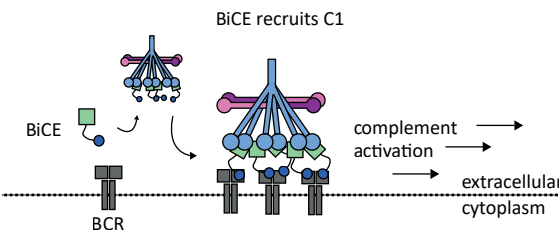
Generation of protein-peptide conjugates

To achieve targeted cell killing of ACPA-expressing B cells, a bispecific construct was generated using nanobody C1qNb75 coupled to the ACPA-binding CCP4 peptide (Figure 1A). As control, conjugates were generated using the CArgP4 peptide, which lacks the citrullinated amino acid and does not bind the ACPA BCR [15]. To generate the constructs, nanobodies were produced with a C-terminal sortag, which allows for incorporation of a Gn-conjugate (Figure 1B) [17]. Since it was unknown if the dimensions of C1 with respect to the ACPA BCR would be sufficiently compatible to accommodate efficient binding of C1, the nanobody was modified with three different linkers to space the peptide from the nanobody: a BC16 linker (16, short flexible), a BC60 linker (60, long flexible) or a dual tandem alpha helix (ta, semi-flexible) [14]. Using sortase A, a GGG-DBCO peptide was conjugated to the nanobody. This step was required due to the fact that the N-terminus of the CCP4 peptide is used in the cyclization process, thus prohibiting the modification of CCP4 with a GGG-repeat at the N-terminus for direct conjugation to C1qNb75, as is usual. Instead, the peptides were synthesized to contain azide moieties on the C-terminus. After incorporation of the GGG-DBCO via the sortase reaction, the peptides were coupled to the nanobody by letting the azide react spontaneously and selectively with the DBCO-C1qNb75. Peptides were added at 2 times excess to the DBCO-modified nanobodies. After overnight coupling, the conjugates were buffer exchanged and concentrated, before conjugation efficiency was evaluated using SDS-PAGE (Figure 1F). Here, a minor shift was observed in conjugate size, which was a positive indication for successful coupling. To confirm incorporation of the peptides, mass spectrometry was performed. The results obtained revealed that constructs were fully conjugated, although a minor amount of intermediates was also present (Supplementary figure 1, Supplementary table 1). Nevertheless, the coupling method was shown to be an effective strategy to couple the peptides to C1qNb75.

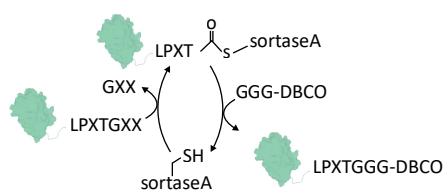
Evaluation of C1qNb75-CCP4 BiCEs on ACPA-expressing Ramos cells

As a proof-of-concept, we initially investigated whether the C1qNb7-CCP4 BiCEs could kill Ramos cells expressing ACPA BCRs. Ramos cells expressing anti-TT BCRs were used as a negative control. In viability assays, we observed reduced conversion of XTT to the bright orange-colored formazan product when ACPA-expressing Ramos cells were incubated with C1qNb75-CCP4 BiCEs, but not with the negative-control C1qNb75-CArgP4 BiCEs, indicating efficient cell killing of ACPA-expressing Ramos cells by C1qNb75-CCP4. Likewise, the anti-TT-expressing Ramos cells were not killed by C1qNb75-CCP4 BiCEs indicating antigen-specific killing of cells. Interestingly, all of the tested linker variants killed the ACPA-expressing Ramos cells to a similar extent. The ability of rituximab to kill both the ACPA-expressing 3F3 cell line as well as the anti-TT-expressing cell line confirmed the sensitivity of all cell lines to complement-dependent killing (Figure 2A). Since the killing capacities of all BiCEs were similar despite their different linkers, we continued using the ta-linked BiCEs in following experiments as it was expressed with better yields compared to the other two nanobody constructs. Next, we wished to determine whether complement-mediated toxicity was responsible for killing of ACPA-expressing Ramos cells by the CCP4-BiCE. To this end, we investigated whether rituximab and C1qNb75-ta-CCP4-induced killing was reduced in the absence of normal human serum (NHS) (Figure 2B) or in presence of the C5

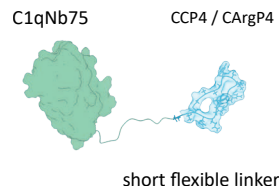
A



B



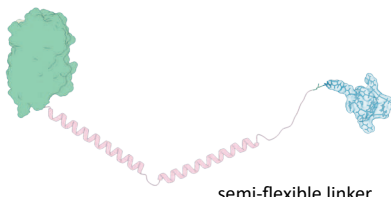
C



D



E



7

F

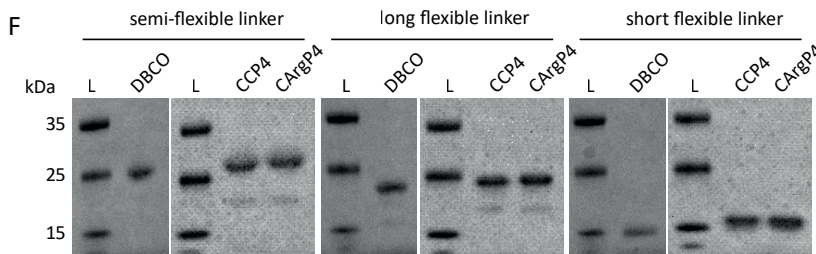
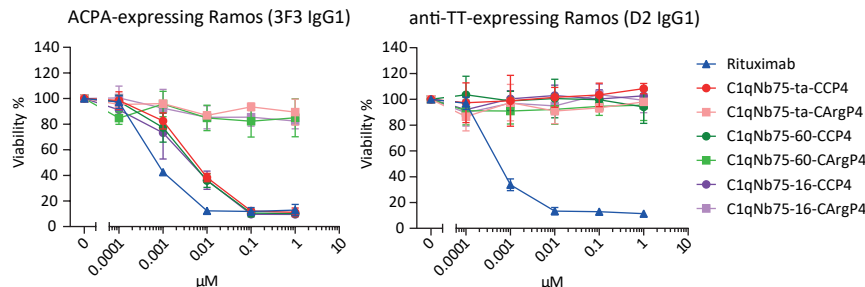


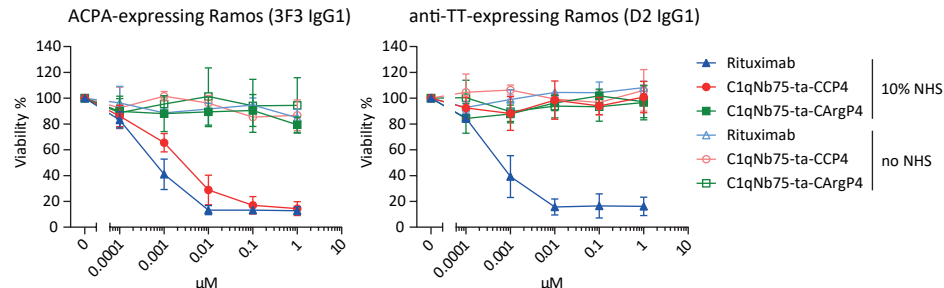
Figure 1. BiCE synthesis. A. C1qNb75-CCP4 BiCE conjugates bind to the ACPA-BCR and C1q simultaneously, thereby locally activating complement. B. The sorttagging mechanism to modify C1qNb75 (green) with a GGG-DBCO peptide (blue). C,D,E. Three analogues were generated with various linker lengths and linker properties: the short, long and semi-flexible linker. F. SDS-PAGE analysis of GGG-DBCO modified (DBCO) and peptide modified (CCP4 and CArgP4) nanobodies. Expected masses after conjugation: short flexible: 16979 Da, long flexible: 20041 Da, semi-flexible: 22573 Da. L is the reference ladder.

inhibitor eculizumab (Figure 2C). These studies revealed no toxicity in absence of NHS or in presence of eculizumab, indicating the complement-mediated cause of toxicity.

A



B



C

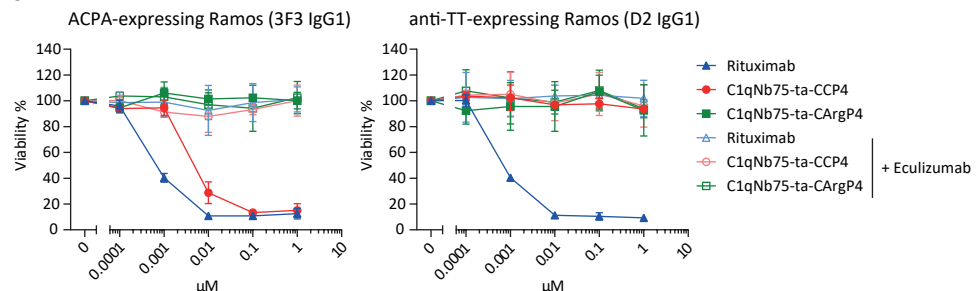


Figure 2. Ramos cell killing by BiCEs. Viability percentages of ACPA-expressing Ramos cells (left) and anti-TT-expressing Ramos cells (right). A. Cell viability after treatment with varying C1qNb75-CCP4/CArgP4 BiCEs or rituximab. B. Cell viability after treatment with C1qNb75-ta-CCP4/CArgP4 in presence or absence of 10% NHS. C. Cell viability after treatment with C1qNb75-ta-CCP4/CArgP4 in presence or absence of eculizumab. All figures show data from three independent experiments. Error bars indicate standard deviations of three experiments.

To extend these findings to other ACPA clones, we subsequently studied the killing efficiency of C1qNb75-ta-CCP4 on a set of different ACPA-expressing Ramos cell lines, encompassing IgG3, IgM and various IgG1 BCRs (Figure 3). Ramos cells expressing no BCR (MDL-AID KO) or an anti-TT BCR were used as negative controls. In parallel, we confirmed BCR expression of all cell lines during the killing experiments (Supplementary figure 2).

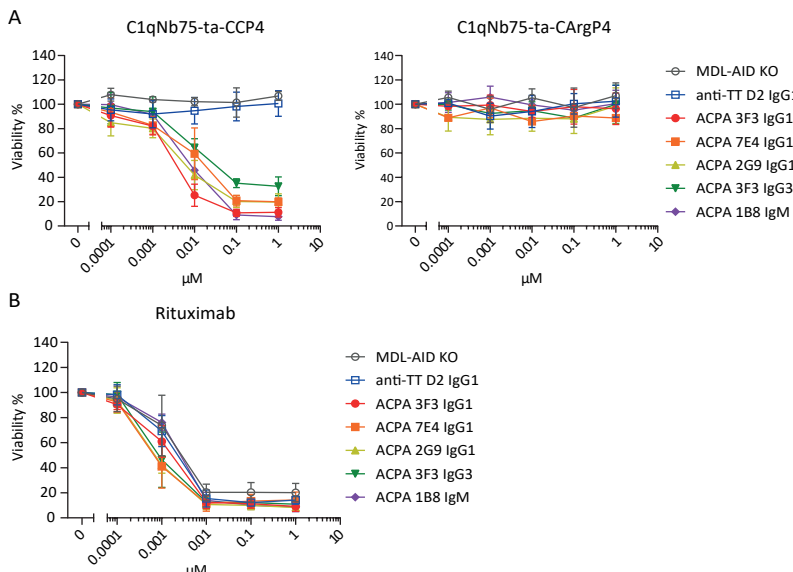


Figure 3. C1qNb75-ta-CCP4 BiCE killing Ramos cells expressing various ACPA BCRs. Viability percentages of Ramos cells expressing ACPA BCRs (3F3 IgG1, 7E4 IgG1, 2G9 IgG1, 3F3 IgG3 and 1B8 IgM), an irrelevant BCR (anti-TT D2 IgG1) or no BCR (MDL-AID KO) after treatment with A. (left) C1qNb75-ta-CCP4, A. (right) C1qNb75-ta-CArgP4 or B. rituximab, all in combination with 10% NHS. Figures show data from three independent experiments. Error bars indicate standard deviations of three experiments.

In ACPA⁺-RA patients, secreted ACPA are present in circulation which, in theory, could block binding of ACPA-expressing B cells to the C1qNb75-CCP4 BiCE. Therefore, we subsequently investigated whether the presence of soluble ACPA could interfere with killing of ACPA-expressing Ramos cells. To this end, we added monoclonal ACPA or plasma derived from RA patients to the BiCE mixtures prior to addition to Ramos cells. Monoclonal antibodies could fully block the BiCE-induced cell death when used in high concentrations (Figure 4A). Similarly, high concentrations of plasma from RA patients with confirmed presence of ACPA-IgG (Figure 4D) could block BiCE-induced cell death (Figure 4B), although this effect could be overcome by increasing the BiCE concentration (Figure 4C).

Evaluation of C1qNb75-ta-CCP4 BiCE on PBMCs-derived from RA patients

Due to the scarcity of ACPA-expressing B cells in RA-patient PBMCs, performing XTT viability assays is not feasible. Therefore, to evaluate the capacity of C1qNb75-ta-CCP4 to kill primary ACPA-expressing B cells in RA patient-derived PBMCs, we used an experimental approach similar to the XTT viability assays, except using antigen-specific flow cytometry as a readout. First, to determine whether this sensitive method could be successfully used to analyze the efficacy of BiCEs, ACPA-expressing Ramos cells (3F3 IgG1) were spiked into healthy donor-derived PBMCs and this cell mixture was incubated with C1qNb75-ta-CCP4/CArgP4 BiCEs in the presence of 10% NHS or 10% heat-inactivated NHS. Subsequent antigen-specific tetramer staining revealed the double-positive (CCP4⁺) diagonal in untreated samples, indicating the presence of ACPA-expressing Ramos cells, whereas in the samples treated with C1qNb75-ta-CCP4 and 10% NHS this diagonal was absent. Importantly, in the condition treated with C1qNb75-ta-CCP4 and 10% heat-inactivated NHS, the CCP4⁺ diagonal was retained indicating that

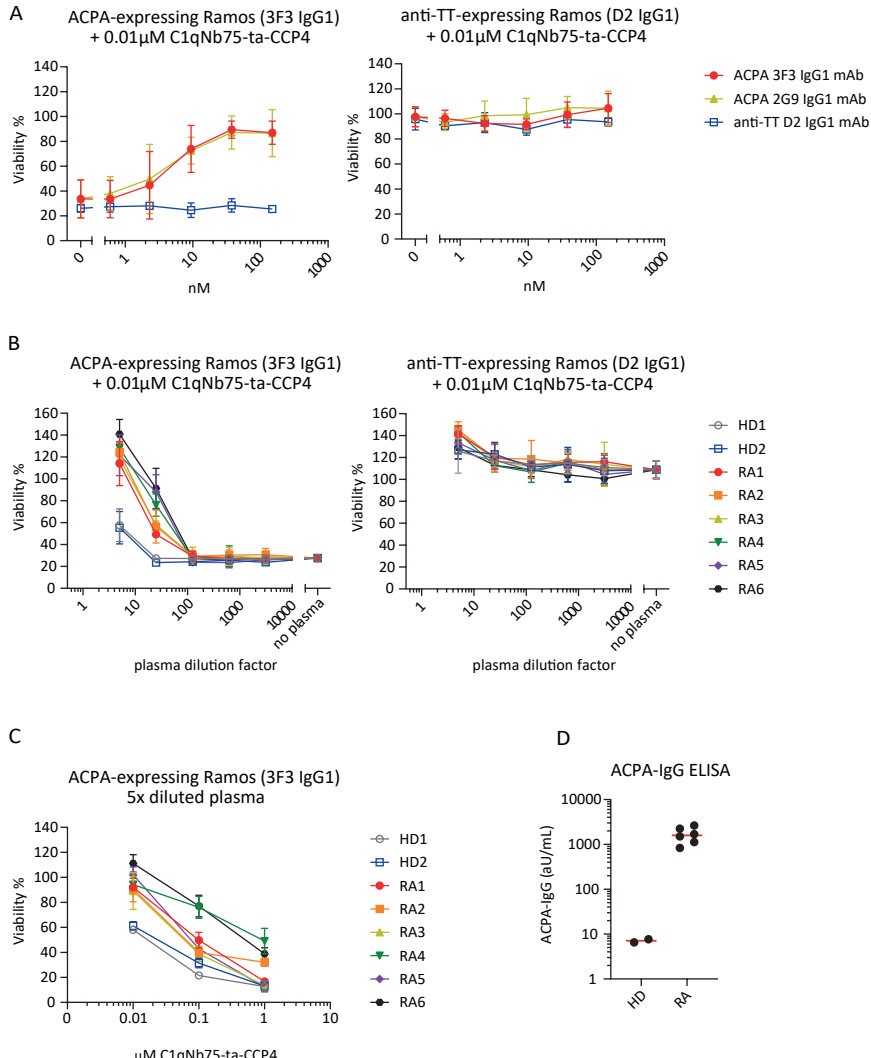


Figure 4. BiCE-induced killing of ACPA-expressing Ramos cells in presence of soluble ACPA. Viability percentages of ACPA-expressing Ramos cells (left) and anti-TT-expressing Ramos cells (right) after treatment with C1qNb75-ta-CCP4 BiCE pre-incubated with A. a titration of monoclonal antibodies, B. with a titration of plasma samples derived from healthy donors (HD1 and HD2) and RA patients (RA1-6), or C. with 5x diluted plasma samples in a titration of C1qNb75-ta-CCP4 conjugate. D. Presence of ACPA-IgG in plasma samples. Figures show data from three independent experiments. Error bars indicate standard deviations of three experiments.

complement inactive serum was not able to mediate cell lysis. Also the samples treated with either C1qNb75-ta-CArgP4 + 10% NHS or C1qNb75-ta-CArgP4 + 10% heat-inactivated NHS retained a clearly visible antigen-specific diagonal (Figure 5). Thus, together, these findings indicate the ability of the C1qNb75-ta-CCP4 BiCE to eradicate ACPA-expressing Ramos cells from healthy donor PBMCs, and demonstrates this flow cytometry method suitable to evaluate efficacy of the BiCEs.

Having determined that C1qNb75-ta-CCP4 in the presence of NHS eradicates ACPA-expressing Ramos cells from healthy donor PBMCs, as indicated by absence of CCP4⁺⁺ staining diagonal, and that heat-inactivated NHS retains this CCP4⁺⁺ diagonal, we next used PBMCs derived from RA patients to delineate whether patient ACPA-expressing B cells were also efficiently targeted by the C1qNb75-ta-CCP4. In PBMC samples from three patients, we compared the presence of ACPA-expressing B cells after treatment with C1qNb75-ta-CCP4 and either 10% NHS or 10% heat-inactivated NHS. We observed an absence or strong decline in ACPA-expressing B cells when incubated with C1qNb75-ta-CCP4 with 10% NHS (Figure 6). In PBMC samples from an additional three patients, we compared ACPA-expressing B cells after treatment with C1qNb75-ta-CCP4 and either 10% autologous serum or 10% heat-inactivated autologous serum. The data obtained indicated a reduction in the number of ACPA-expressing B cells when cells were

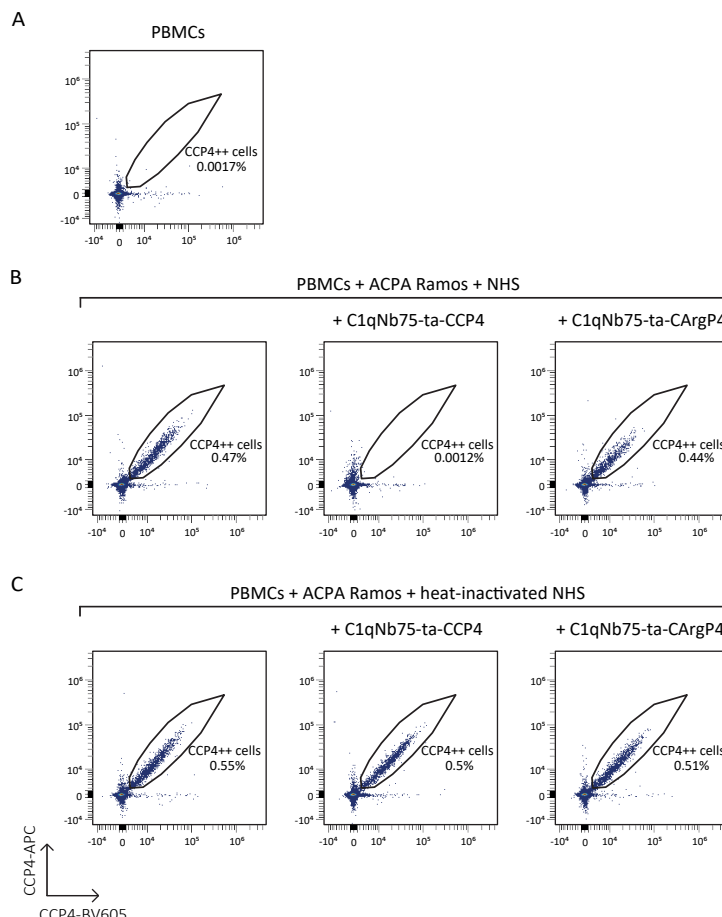


Figure 5. BiCE-induced absence of ACPA-expressing Ramos cells spiked into healthy donor PBMCs. A. PBMCs showing no ACPA-expressing Ramos cells B. ACPA-expressing (3F3 IgG1) Ramos cells spiked into PBMCs, treated with 10% NHS (left), C1qNb75-ta-CCP4 and 10% NHS (middle) or C1qNb75-ta-CArgP4 and 10% NHS (right). C. ACPA-expressing (3F3 IgG1) Ramos cells spiked into PBMCs, treated with 10% heat-inactivated NHS (left), C1qNb75-ta-CCP4 and 10% heat-inactivated NHS (middle) or C1qNb75-ta-CArgP4 and 10% heat-inactivated NHS (right).

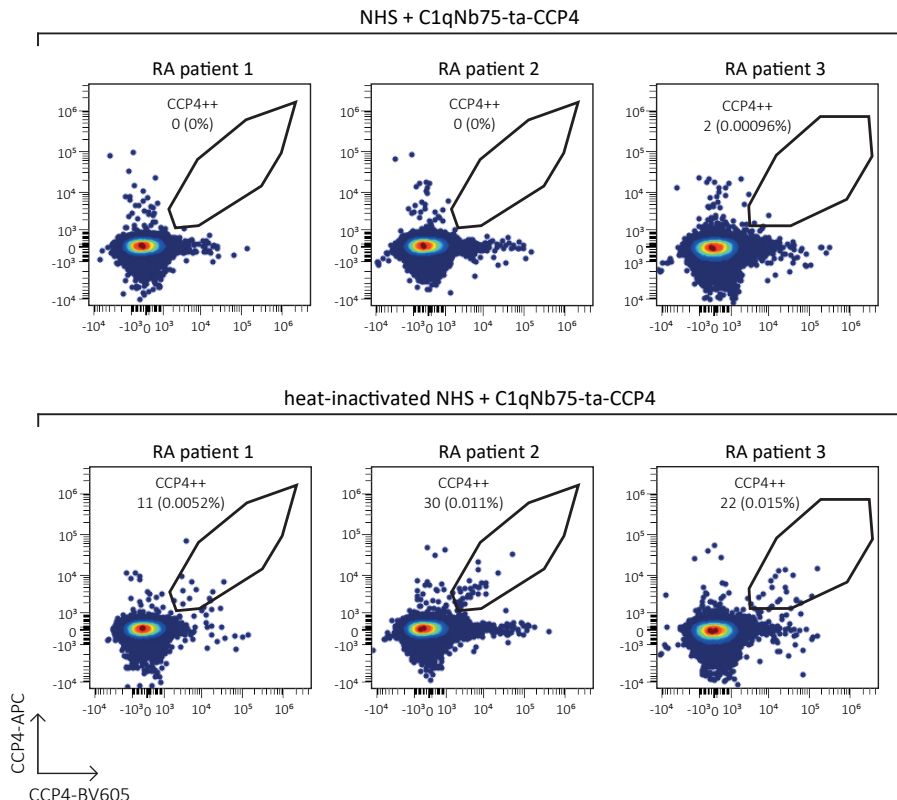


Figure 6. BiCE-induced absence of ACPA-expressing B cells in PBMCs derived from RA patients using NHS. PBMCs from three patients incubated with C1qNb75-ta-CCP4 either with 10% NHS or 10% heat-inactivated NHS. ACPA-expressing B cells are gated as CCP4⁺⁺ cells. Total number of ACPA-expressing B cells and percentage from total CD19⁺ B cells are indicated. The gating strategy is depicted in Supplementary figure 3.

incubated in presence of autologous serum as compared to heat-inactivated autologous serum (Figure 7). From all six RA patients, several B-cell subsets were analyzed and none showed a clear difference after incubation with C1qNb75-ta-CCP4 in combination with active versus heat-inactivated serum, except for the antigen-specific ACPA-expressing B-cell population which was, in all cases, reduced in number (Supplementary figure 4).

To further substantiate the findings that ACPA-expressing B cells are specifically eradicated from RA patient-derived PBMCs, we next investigated whether adding eculizumab to BiCE treatment would retain the CCP4⁺⁺ diagonal when performing the CCP4 tetramer staining. To this end, we mixed ACPA-expressing Ramos cells (3F3 IgG1), which are GFP⁺, with Ramos cells not expressing a BCR (MDL-AID KO) which are GFP⁻. After adding the C1qNb75-ta-CCP4 BiCE with 10% NHS in presence or absence of eculizumab, CCP4 tetramer staining revealed that, unexpectedly, the CCP4⁺⁺ diagonal was not retained in presence of eculizumab whereas, similar to previous experiments, heat-inactivation of NHS did cause retention of the CCP4⁺⁺ diagonal. However, as was observed based on the forward- and sideward scatters as well as the GFP signal, ACPA-expressing Ramos cells are in fact still

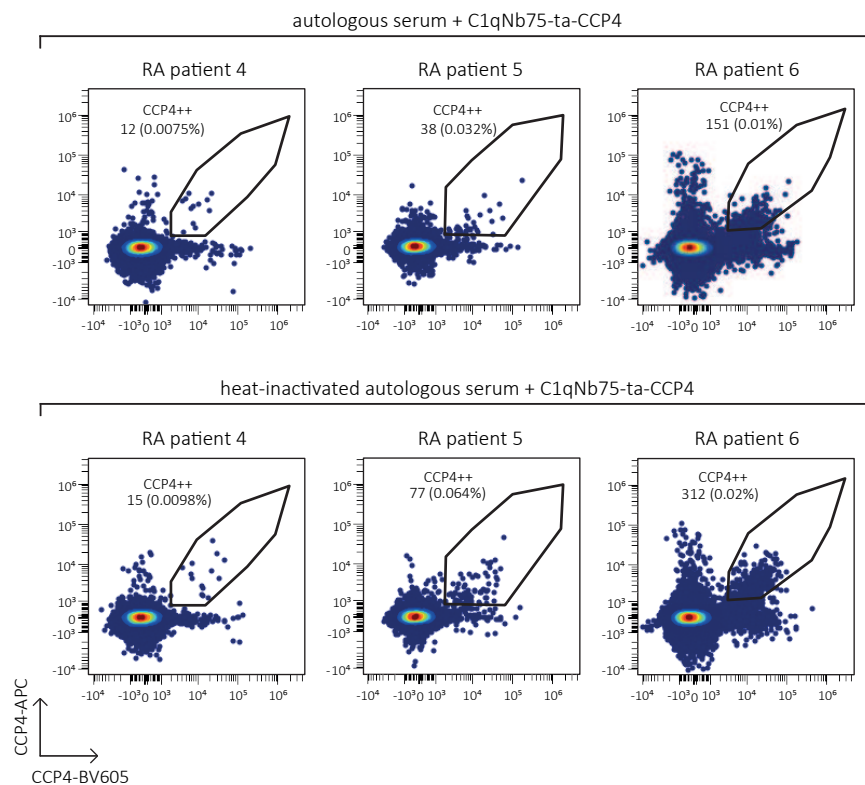
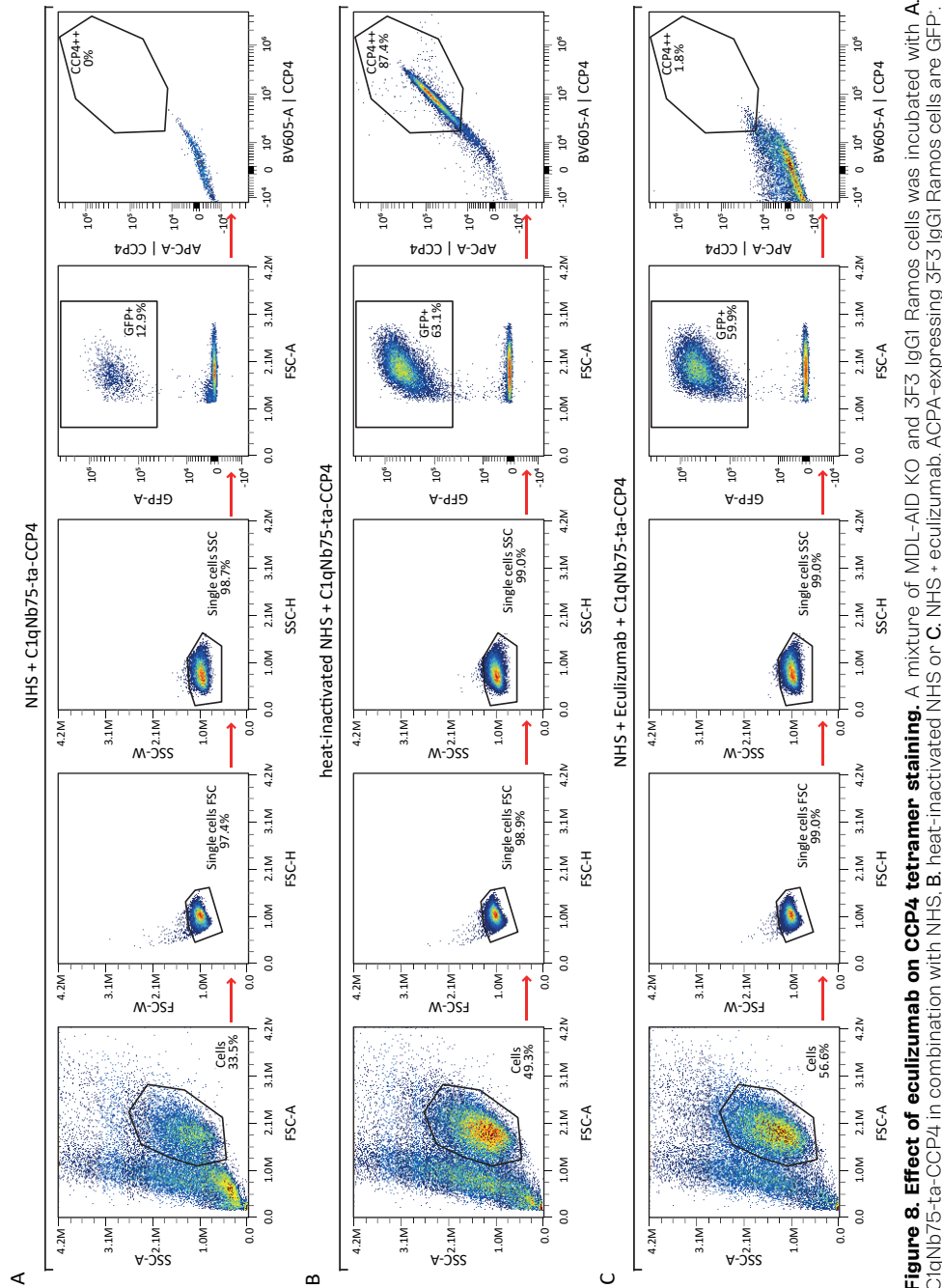


Figure 7. BiCE-induced decrease of ACPA-expressing B cells in PBMCs derived from RA patients using autologous serum. PBMCs from three patients incubated with C1qNb75-ta-CCP4 either with 10% autologous serum or 10% heat-inactivated autologous serum. ACPA-expressing B cells are gated as CCP4⁺⁺ cells. Total number of ACPA-expressing B cells and percentage from total CD19⁺ B cells are indicated. The gating strategy is depicted in Supplementary figure 3.

present in the cell mixture, indicating that the CCP4 tetramer staining may somehow be hindered. As these data were unexpected and possibly explained by interference of C1 present in complement-active serum in the visualization of ACPA-expressing B cells, we cannot exclude that ACPA-expressing cells are still present in PBMC samples after treatment with CCP4-BiCEs.



Discussion

Autoreactive B cells play a central role in many AIDs, including RA. In particular, disease-specific ACPA-expressing B cells have been implicated in RA pathogenesis [4], and their persistently activated phenotype, even in patients in clinical remission [6], suggests that their targeted depletion could aid in accomplishing sustained disease control. In this study, we present a strategy for the selective depletion of ACPA-expressing B cells to silence the ACPA B-cell response and achieve immunological remission. Our approach entails the use of BiCEs consisting of CCP4, a ligand for ACPA-expressing B cells, conjugated to the anti-C1q nanobody C1qNb75 [11]. We evaluated the efficacy of these BiCEs using both engineered Ramos B-cell lines expressing ACPA BCRs and PBMCs from ACPA-positive RA patients.

We evaluated three different BiCE constructs varying in linker between C1qNb75 and CCP4, as we hypothesized that linker flexibility and distance to the cell membrane could influence complement-mediated cytotoxicity. However, all CCP4 containing BiCE variants efficiently induced cytotoxicity in multiple ACPA-expressing Ramos cell lines, independent of linker composition. Excluding NHS or including eculizumab confirmed that BiCE-mediated killing was complement-dependent. Moreover, all currently analyzed Ramos cell lines showed sensitivity to C1qNb75-ta-CCP4-induced killing. Interestingly, the 3F3 IgG3 ACPA-expressing Ramos cell line exhibited slightly reduced sensitivity. This effect may be attributed to the longer hinge region of IgG3, increasing the distance between the BiCE and the cell membrane, potentially leading to less efficient MAC-pore formation [14, 18, 19].

One potential hurdle in antigen-specific therapy is interference by circulating antibodies targeting the same antigen. Indeed, we observed that both monoclonal ACPA and polyclonal ACPA present in patient-derived plasma can hinder BiCE-mediated killing of target Ramos cells, indicating plasmapheresis may be required prior to dosing. However, given the observation that the inhibitory effect of ACPA in plasma was mostly diminished by increasing the BiCE dosage, dose optimization might circumvent the need of plasmapheresis [20]. Nevertheless, the possibility of excessive immune complex formation and C1 depletion requires further investigation. Although the *in vivo* half-life of C1qNb75-ta-CCP4 remains to be investigated, the strong binding affinity of C1qNb75 to C1 suggests that C1qNb75-ta-CCP4 will mainly circulate in complex with C1 [11]. Consequently, its clearance is likely to mirror that of C1, suggesting that C1 depletion is unlikely to be a long-term issue [21]. Moreover, nanobodies typically exhibit short half-lives of hours, suggesting that any unbound nanobody present if administered in high doses, is expected to be cleared rapidly [22].

To validate our findings in primary ACPA-expressing B cells, we tested C1qNb75-ta-CCP4 BiCEs on PBMCs from ACPA-positive RA patients. Antigen-specific CCP4-tetramer staining revealed a reduction in ACPA-expression B cells upon incubation with BiCEs in the presence of 10% NHS, compared to 10% heat-inactivated NHS. Similar results were observed using autologous serum, although the decrease in ACPA-expressing B cells was less pronounced in these experiments as compared to the studies using NHS samples. This is likely due to the presence of secreted ACPA in autologous serum. Importantly, other B-cell subsets remained unaffected

under both serum conditions, emphasizing the specificity of the approach.

The experiments using eculizumab in antigen-specific stainings provided further insight on the interpretation of these results. Although forward- and sideward scatters as well as GFP signal indicated survival of the ACPA-expressing Ramos cells when eculizumab was added, the CCP4⁺⁺ staining diagonal was not retained. This finding raises two potential interpretations: (1) the observed decline in ACPA-expressing B cells may reflect complement-mediated cell killing, consistent with viability assays in Ramos cell lines, or (2) the staining signal may be blocked either by the BiCE, potentially resulting from BiCE multimerization upon C1q binding, or perhaps by C3 deposition, which still takes place in presence of eculizumab but not in heat-inactivated serum. However, the latter hypothesis is challenged by the observation that the CCP4⁺⁺ staining diagonal persists in heat-inactivated NHS, where C1 is still present but inactive due to C1r and C1s inactivation. Nonetheless, further experiments are required to test efficacy in patient material, e.g. by culturing the cells after BiCE treatment to subsequently analyze ACPA production as a proxy for survival of ACPA-expressing B cells.

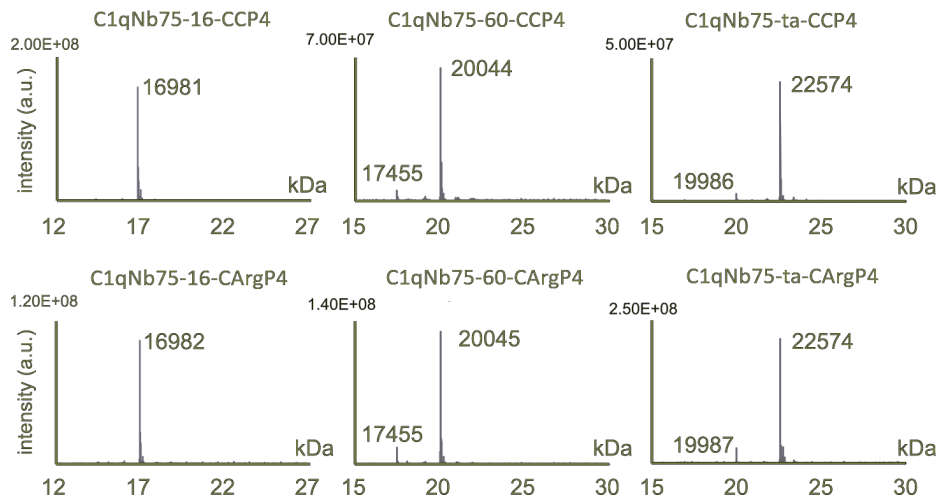
In conclusion, we demonstrate the feasibility of C1qNb75-CCP4 BiCEs to selectively deplete ACPA-expressing B cells. This antigen-specific treatment modality holds promise for scalable, off-the-shelf therapeutic applications and offers an attractive alternative to expensive, tailor-made approaches such as CAR-T-cell therapy. Moreover, the modular design of BiCEs allows for adaptation to other autoantibody-driven diseases, making BiCEs a versatile tool for targeted immunotherapy in the context of AIDs.

Author contributions

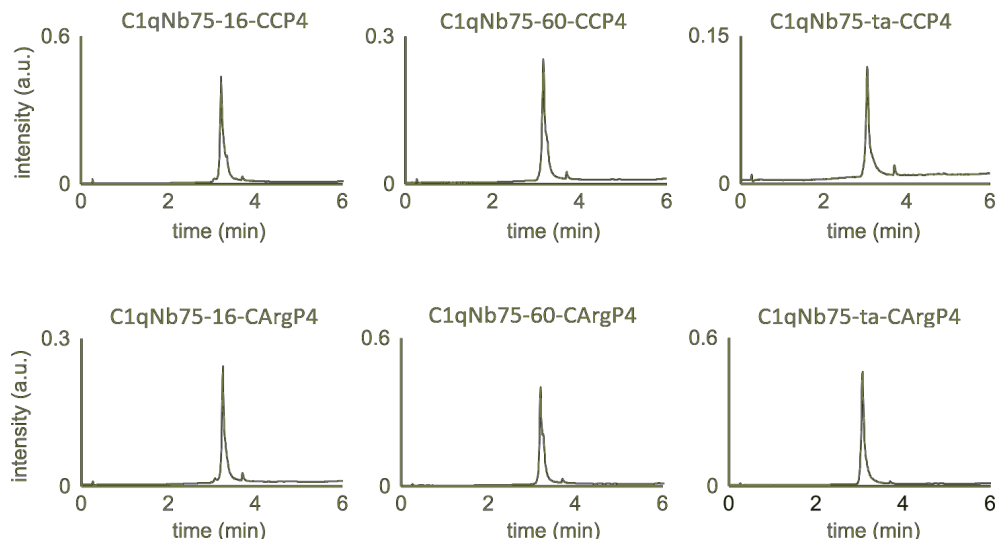
SK: involved in experimental design, performed cellular assays, wrote the manuscript. SMWRH: involved in experimental design, performed synthesis and characterization of C1qNb75-CCP4 BiCEs. LAT: involved in experimental design. REMT, THS: involved in project supervision and experimental design.

References

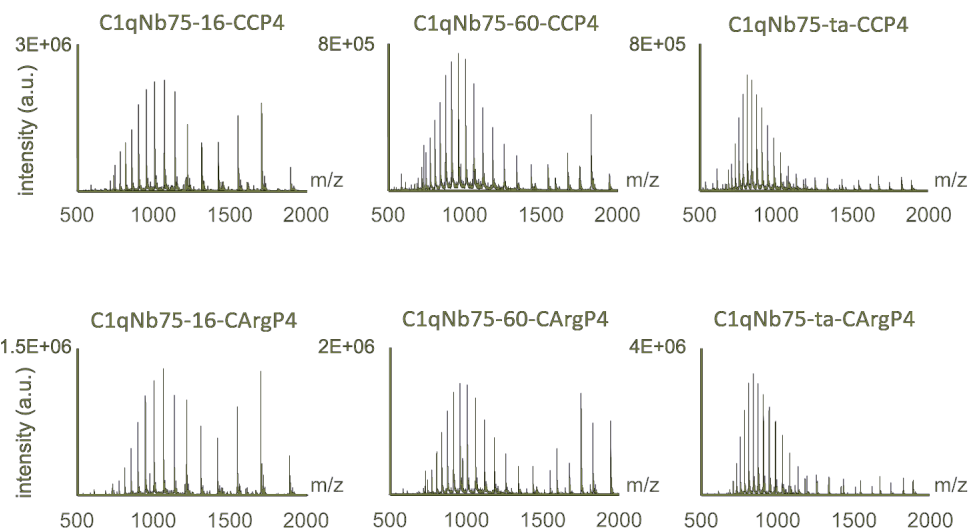
1. Holborough-Kerkvliet, M.D., et al, Addressing the key issue: Antigen-specific targeting of B cells in autoimmune diseases. *Immunol Lett*, 2023. 259: p. 37-45.
2. Volkov, M., Comprehensive overview of autoantibody isotype and subclass distribution. *J Allergy Clin Immunol*, 2022. 150(5): p. 999-1010.
3. Edwards, J.C.W. and G. Cambridge, Sustained improvement in rheumatoid arthritis following a protocol designed to deplete B lymphocytes. *Rheumatology*, 2001. 40: p. 205-211.
4. Scherer, H.U., D. van der Woude, and R.E.M. Toes, From risk to chronicity: evolution of autoreactive B cell and antibody responses in rheumatoid arthritis. *Nat Rev Rheumatol*, 2022. 18(7): p. 371-383.
5. van der Helm-van Mil, A.H., et al, Antibodies to citrullinated proteins and differences in clinical progression of rheumatoid arthritis. *Arthritis Res Ther*, 2005. 7(5): p. R949-58.
6. Kristyanto, H., et al, Persistently activated, proliferative memory autoreactive B cells promote inflammation in rheumatoid arthritis. *Science Translational Medicine*, 2020. 12.
7. Neppelenbroek, S., et al, Autoreactive B cells remain active despite clinical disease control in rheumatoid arthritis. *J Autoimmun*, 2024. 149: p. 103320.
8. Kroos, S., et al, Increased Phosphorylation of Intracellular Signaling Molecules Indicates Continuous Activation of Human Autoreactive B-Cells. *Eur J Immunol*, 2025. 55(1): p. e202451361.
9. Edwards, J.C.W., et al, Efficacy of B-Cell-Targeted Therapy with Rituximab in Patients with Rheumatoid Arthritis. *The New England Journal of Medicine*, 2004. 350.
10. Smith, M.R, Rituximab (monoclonal anti-CD20 antibody): mechanisms of action and resistance. *Oncogene*, 2003. 22(47): p. 7359-68.
11. Laursen, N.S., et al, Functional and Structural Characterization of a Potent C1q Inhibitor Targeting the Classical Pathway of the Complement System. *Front Immunol*, 2020. 11: p. 1504.
12. Pedersen, D.V., et al, Bispecific Complement Engagers for Targeted Complement Activation. *J Immunol*, 2023. 211(3): p. 403-413.
13. Pedersen, M.L., et al, Nanobody-mediated complement activation to kill HIV-infected cells. *EMBO Mol Med*, 2023. 15(4): p. e16422.
14. Hamers, S., A.L. Boyle, and T.H. Sharp, Engineering Agonistic Bispecifics to Investigate the Influence of Distance on Surface-Mediated Complement Activation. *J Immunol*, 2024. 213(2): p. 235-243.
15. Kissel, T., et al, Antibodies and B cells recognising citrullinated proteins display a broad cross-reactivity towards other post-translational modifications. *Ann Rheum Dis*, 2020. 79(4): p. 472-480.
16. Kerkman, P.F., et al, Identification and characterisation of citrullinated antigen-specific B cells in peripheral blood of patients with rheumatoid arthritis. *Ann Rheum Dis*, 2016. 75(6): p. 1170-6.
17. Guimaraes, C.P., et al, Site-specific C-terminal and internal loop labeling of proteins using sortase-mediated reactions. *Nat Protoc*, 2013. 8(9): p. 1787-99.
18. Cleary, K.L.S., et al, Antibody Distance from the Cell Membrane Regulates Antibody Effector Mechanisms. *J Immunol*, 2017. 198(10): p. 3999-4011.
19. Abendstein, L., et al, Complement is activated by elevated IgG3 hexameric platforms and deposits C4b onto distinct antibody domains. *Nat Commun*, 2023. 14(1): p. 4027.
20. Suwannalai, P., et al, Anti-citrullinated protein antibodies have a low avidity compared with antibodies against recall antigens. *Ann Rheum Dis*, 2011. 70(2): p. 373-379.
21. An, G., Concept of Pharmacologic Target-Mediated Drug Disposition in Large-Molecule and Small-Molecule Compounds. *J Clin Pharmacol*, 2020. 60(2): p. 149-163.
22. Liu, L., et al, Nanobody-based drug delivery systems for cancer therapy. *J Control Release*, 2025. 381: p. 113562.



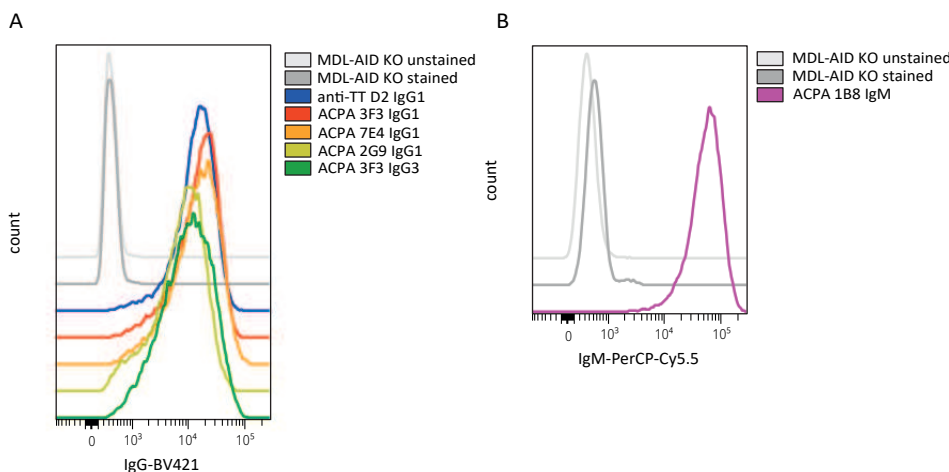
Supplementary figure 1. Deconvoluted masses from the ion count chromatograms and m/z data displayed in supplementary figures 2 and 3. See supplementary table 1 for expected masses of each intermediate.



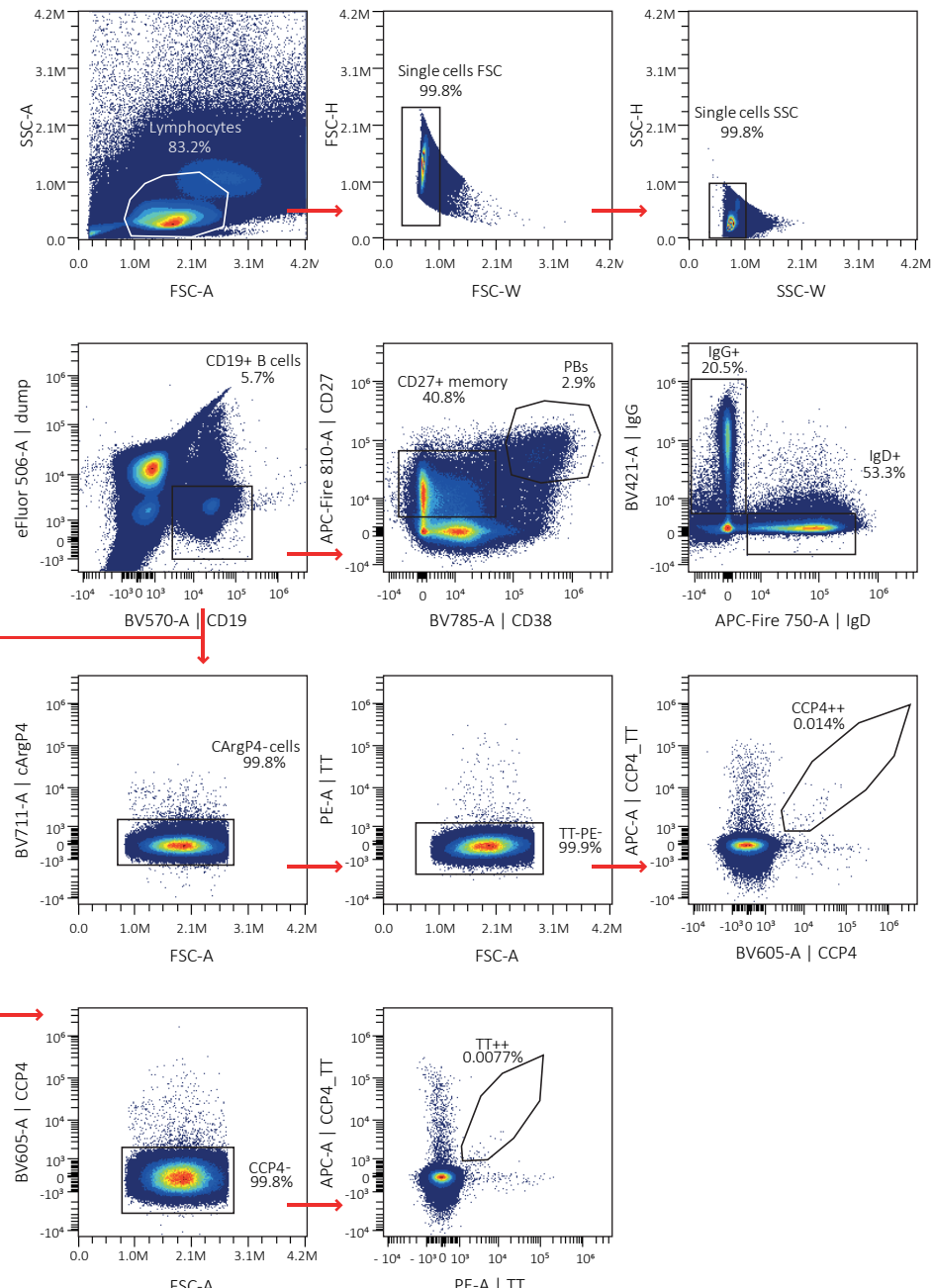
Supplementary figure 2. Ion count chromatograms of nanobody conjugates.



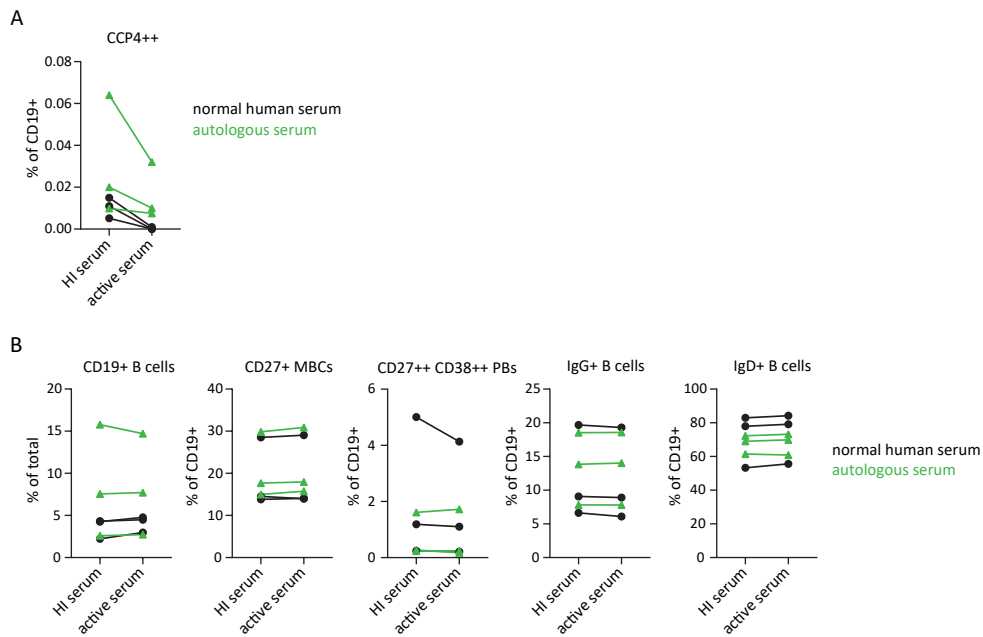
Supplementary figure 3. *m/z* data of nanobody conjugates.



Supplementary figure 4. BCR expression on Ramos cell lines. Histograms indicate the level of membrane-bound A. IgG or B. IgM on the Ramos cell lines used in viability experiments. Figures are representative for three independent measurements performed on the same day as viability assays.



Supplementary figure 5. Gating strategy PBMCs. Lymphocyte gate is set based on FSC-A and SSC-A. Note that this gate is set much broader in the case of experiments where Ramos cells were spiked in, as these cells are bigger in size compared to regular lymphocytes. After two single cell gates (based on FSC and SSC), CD19+ B cells are gated. From this population, several B-cell subsets are gated. Additionally, from the CD19+ cells, CArgP4+ cells are selected to gate CCP4++ cells and TT++ cells.



Supplementary figure 6. Histograms depicting B cell subsets in RA patient PBMCs. PBMCs derived from ACPA-positive RA patients were treated with ClqNb75-ta-CCP4 and NHS or heat-inactivated NHS (black), or treated with ClqNb75-ta-CCP4 and autologous serum or heat-inactivated autologous serum (green).

Supplementary table 1. Expected masses of the BiCEs in Daltons. CCP4 and CArgP4 have the same mass and thus conjugates are expected to have the same mass. The intermediate is the conjugate with the GGG-DBCO peptide attached.

	Starting material	Hydrolysis product	Intermediate	Product
Short flexible linker (16)	30704.8	14393.8	14992.4	16979.0
Long flexible linker (60)	33767.6	17456.6	18055.2	20041.8
Semi-flexible linker (ta)	25096.1	19987.8	20586.4	22573.0

Supplementary table 2. Patient characteristics

Characteristic	RA patients (n = 6)
Age, years*	67 (58 – 75)
Female, n (%)	4 (67%)
CCP4-IgG (aU/mL)*	1596 (1055 – 2342)
DAS28(3v)*	2,9 (1,6 – 3,6)
28 swollen joint count*	0 (0 – 1,3)
28 tender joint count*	0 (0 – 1)
Erythrocyte sedimentation rate (mm/hr)*	33,5 (8,8 – 41,3)
Current treatment	
Methotrexate, n	5
Hydroxychloroquine, n	1
Sulfasalazine, n	1
Leflunomide, n	1

*Values represent median (interquartile range). RA, rheumatoid arthritis.

DAS, disease activity score. n/a, not applicable

